



# THE UNIVERSITY *of* EDINBURGH

## Edinburgh Research Explorer

### **Piezoelectric sensing of electrothermally actuated silicon carbide MEMS resonators**

**Citation for published version:**

Svilli, B, Mastropaolo, E & Cheung, R 2014, 'Piezoelectric sensing of electrothermally actuated silicon carbide MEMS resonators' *Microelectronic Engineering*, vol. 119, pp. 24-27. DOI: 10.1016/j.mee.2014.01.007

**Digital Object Identifier (DOI):**

[10.1016/j.mee.2014.01.007](https://doi.org/10.1016/j.mee.2014.01.007)

**Link:**

[Link to publication record in Edinburgh Research Explorer](#)

**Document Version:**

Peer reviewed version

**Published In:**

Microelectronic Engineering

**General rights**

Copyright for the publications made accessible via the Edinburgh Research Explorer is retained by the author(s) and / or other copyright owners and it is a condition of accessing these publications that users recognise and abide by the legal requirements associated with these rights.

**Take down policy**

The University of Edinburgh has made every reasonable effort to ensure that Edinburgh Research Explorer content complies with UK legislation. If you believe that the public display of this file breaches copyright please contact [openaccess@ed.ac.uk](mailto:openaccess@ed.ac.uk) providing details, and we will remove access to the work immediately and investigate your claim.



**NOTICE:** this is the author's version of a work that was accepted for publication in *Microelectronic Engineering*. Changes resulting from the publishing process, such as peer review, editing, corrections, structural formatting, and other quality control mechanisms may not be reflected in this document. Changes may have been made to this work since it was submitted for publication. A definitive version was subsequently published in *Microelectronic Engineering*, [VOL 119, PP. 24-27, (2014)] DOI:10.1016/j.mee.2014.01.007

## **Piezoelectric Sensing of Electrothermally Actuated Silicon Carbide MEMS Resonators**

Boris Sviličić<sup>a)</sup>, Enrico Mastropaolo, Rebecca Cheung

Institute for Integrated Micro and Nano Systems, The University of Edinburgh, West Mains Road, Edinburgh EH9  
3JF, United Kingdom

a) Permanent position: Department of Marine Electronics and Communications, Faculty of Maritime Studies,  
University of Rijeka, Studentska ulica 2, HR-51000 Rijeka, Croatia

E-mail: svilicic@pfri.hr; Tel.: +385 98 529 550

### **Abstract**

The influence of piezoelectric sensor design on electrothermally actuated micro-electro-mechanical (MEMS) resonators performance (resonant frequency and Q factor) has been investigated. Silicon-carbide double-clamped beam resonators have been fabricated with platinum electrothermal actuator and lead-zirconium-titanate piezoelectric sensor on the top of the beam. The fabricated devices differ only in the piezoelectric sensor length, while other dimensions and technological parameters are the same. The 200  $\mu\text{m}$  long devices resonate between 0.6 and 1.1 MHz with Q factor in air up to 410, and can be tuned up to 300,000 ppm using relatively low DC bias voltages (2 - 6 V). The transmission frequency response measurements have shown that the devices, actuated in the same operating conditions, with shorter piezoelectric sensor resonate at higher frequencies with higher Q factors. However, the wider frequency tuning range has been obtained with devices with longer piezoelectric sensor integrated and positioned closer to the centre of the beam.

**Keywords:** MEMS resonator, silicon carbide, piezoelectric sensing, electrothermal actuation, tuning

## I. INTRODUCTION

Micro-electro-mechanical systems (MEMS) resonators are a potential alternative to filter components and quartz crystal currently used in high-end electronic systems due to their small size and low operating voltages [1]. Among all transduction techniques for electrical induction of mechanical vibrations, major advantages of electrothermal actuation include simple fabrication process, low actuation voltages and impedance matching. Several electrothermally actuated MEMS resonators have been reported in literature, showing high resonant frequencies, high quality (Q) factors and wide frequency tuning ranges [2–5]. Silicon carbide (SiC) is one of the most promising materials for the development of high efficient MEMS resonators due to its excellent mechanical properties [6]. In addition, high thermal conductivity makes it particularly suitable for electrothermal actuation purposes.

Practical implementation of MEMS resonators requires electrical sensing of mechanical vibrations. Recently, we have demonstrated the piezoelectric sensing of an electrothermally actuated and tuned MEMS resonator [5]. The use of piezoelectric transduction for electrical sensing enables stronger electromechanical coupling and better impedance matching compared to the alternative electrostatic transduction [7]. In addition, the fabrication process for the piezoelectric transducers can be controlled better than the electrostatic case, since the stringent nanometric control of the electrode-to-resonator gap spacing is not required. However, the design of the piezoelectric transducer on top of a resonator can significantly affect the resonant performance.

In this work, piezoelectric sensors with different dimensions have been integrated on the top of SiC double-clamped beams (bridge structure) for the study of the influence of

piezoelectric sensor design on device performance. By performing two-port measurements of devices' transmission frequency response, the resonant frequency, Q factor and frequency tuning range as a function of the piezoelectric sensor length have been investigated. Q factor and frequency tuning range dependences on the piezoelectric sensor length have been studied under different DC bias conditions, while resonant frequency dependence has been studied under equilibrium conditions.

## II. TRANSDUCTIONS PRINCIPLES AND DEVICE OPERATION

Electrothermal actuation is a transduction mechanism based on the Joule heating and thereby thermal expansion of a material. The structure of our devices is bimorph meaning that a heating Pt layer (electrothermal actuation electrode) is deposited on an 3C-SiC layer. By applying a voltage across the electrothermal electrode, electric current is dissipated through the electrode resistance. The generated heat induces a temperature gradient within the structure leading to the thermal expansion of the entire structure and therefore to a mechanical strain. The mechanical strain is enhanced by using two materials with different thermal expansion coefficients [8]. Due to square relationship between dissipated power and voltage, the application of an actuation voltage with only AC component and the frequency  $f_{AC}$  can drive a device into resonance if the value of  $f_{AC}$  is equal to the half of the structure's natural frequency  $f_0$  ( $f_{AC}=f_0/2$ ) [9]. In order to drive a device into resonance using the actuation frequency equal to the structure's natural frequency ( $f_{AC}=f_0$ ), the actuation signal should contain both AC and DC components.

Piezoelectricity has been used as a transduction technique for electrical sensing of our devices' operation. Piezoelectricity refers to the property of a material to become electrically

polarized when subjected to mechanical strain. In our devices, the piezoelectric layer is placed on the top of the 3C-SiC beam. When the device is electrothermally driven into resonance, the beam vibrates in vertical direction inducing mechanical strain in the top piezoelectric layer. As a consequence, an alternating voltage with a frequency equal to the frequency of the mechanical vibrations can be detected across the piezoelectric material of the output port.

### **III. EXPERIMENTAL DETAILS**

#### **A. Device design**

The devices have been designed as a two-port double-clamped beam resonator with the beam length of 200  $\mu\text{m}$  and width of 50  $\mu\text{m}$ . The electrothermal actuator has been designed with two platinum (Pt) arms, parallel to the longer side of the beam, connected by a perpendicular arm (u-shaped layout). The electrothermal actuator length is 67  $\mu\text{m}$  (a third of the beam length), the arms' width is 20  $\mu\text{m}$  and the spacing between arms is 3  $\mu\text{m}$ . The strong electromechanical coupling offered by the electrothermal transduction allows the structure to be driven efficiently into vibration by positioning the electrothermal actuator close the beam's root, leaving enough area on the other side of the beam for the piezoelectric sensor. The piezoelectric sensor is formed from a lead-zirconium-titanate (PZT) layer sandwiched between two Pt layers. PZT has been used due to its high piezoelectric coefficient, so that the electromechanical coupling in the sensing part is enhanced [7]. Figure 1 shows a scanning electron micrograph of one of the fabricated devices, and the top and the side view schematics of the designed devices.

#### **B. Fabrication**

The fabrication process consists of three major phases: all layers deposition, electrodes forming and the beam forming. The all layer deposition phase starts with a 2  $\mu\text{m}$  thick 3C-SiC epilayer grown on 4 inch Si wafer [10]. A 100 nm thick silicon dioxide ( $\text{SiO}_2$ ) passivation layer has been grown thermally and a 10 nm thick titanium (Ti) adhesion layer has been deposited on top of the  $\text{SiO}_2$ . The Pt/PZT/Pt stack has been deposited with thicknesses of 100/500/100 nm, respectively [11]. In the second phase, the electrodes have been defined photolithographically. The Pt and Ti layers have been dry etched while the PZT has been wet etched [12]. After patterning the electrodes, a 3  $\mu\text{m}$  thick  $\text{SiO}_2$  layer has been deposited for masking the 3C-SiC layer. The 3C-SiC beam shape has been patterned photolithographically and the exposed  $\text{SiO}_2$  has been dry etched. Afterwards, 3C-SiC beam has been etched and released with inductively-coupled-plasma [13] and  $\text{XeF}_2$  chemical etching.

### **C. Measurement setup**

The fabricated devices have been tested with a RF probe station and the transmission frequency response has been measured by an HP 8753C vector network analyzer. Signal-ground (SG) probes have been used and two-port short-open-load-through (SOLT) calibration has been performed before starting the measurements. The devices under test have been directly connected to the network analyzer without any external interface electronics. In order to perform electrothermal actuation and resonant frequency tuning, the AC signal applied with the network analyzer has been superimposed to a DC voltage provided by an external stabilized DC power. The bottom metal contact of the output electrode has been grounded, while the top metal contact has been used for piezoelectric sensing. All measurements have been performed in air, at room temperature and pressure.

## IV. RESULTS AND DISCUSSION

Testing of the devices has been performed by measuring the transmission frequency response in atmospheric conditions (Figure 2a). The devices under test differ only in the piezoelectric sensor length, while other dimensions and technological parameters are the same. In order to perform a comparative study, the devices measured in this work have been taken from the same die ( $0.7 \text{ cm}^2$ ) and therefore fabrication related differences such as film thicknesses have been minimised.

### A. Piezoelectric port length influence on resonant frequency

The resonant frequency measured as a function of the piezoelectric sensor length is shown on Figure 2b. Resonant frequencies in the range of 0.85 – 1.05 MHz have been measured for the devices actuated with input signal power of 10 dBm and DC bias voltage of 3 V. By decreasing the piezoelectric sensor length from 125  $\mu\text{m}$  to 25 $\mu\text{m}$ , the resonant frequency increases by ~20 kHz (~24,000 ppm). The observed increase of the resonant frequency as the piezoelectric sensor length decreases can be attributed to the decrease of the structure's effective mass. The resonant frequency of a multi-layer bridge resonator is proportional to ratio of the effective spring constant (dependent on Young's modulus and dimensions of the layers) and the effective mass of the structure (dependent on densities and dimensions of the layers). By increasing the piezoelectric sensor length, the effective spring constant increases together with the structure's effective mass. It is believed that the resonant frequency is affected more strongly by the change in the structure's effective mass than by the change in the effective spring constant, and therefore the resonant frequency increases with the piezoelectric sensor length decrease.

## **B. Piezoelectric port length influence on Q factor**

The ratio between the stored energy and the dissipated energy (Q factor) of the devices can be improved by varying the piezoelectric sensor length. Figure 3 shows the Q-factor, calculated as the ration of the resonant frequency and the bandwidth of 3 dB transmission magnitude drop, for piezoelectric sensor lengths of 25, 50 and 100  $\mu\text{m}$  as a function of applied DC bias voltage. The tested devices have been actuated with a constant input AC signal power of 10 dBm while the DC bias voltage has been swept in the range of 2 V - 6 V with step of 1 V. With a DC bias voltage increase, the Q factor in air has been shown to increase for all piezoelectric sensor lengths investigated. In particular, as the DC bias voltage is increased from 2 V to 6 V, the Q factor increases from  $\sim 120$  to  $\sim 350$  and from  $\sim 170$  to  $\sim 410$  for devices with the piezoelectric sensor length of 100  $\mu\text{m}$  and 25  $\mu\text{m}$  respectively. The increase of Q factor obtained with DC bias voltage increase can be attributed to the increase of the vibration amplitude caused by the increase of the generated heat [9]. Since the stored energy is proportional to vibration amplitude squared, the increase of the vibration amplitude induced by the DC bias voltage increase leads to higher Q factor. At fixed DC bias voltage, the Q factor has been shown to increase as the piezoelectric sensor length has been decreased. As shown in Figure 3, with the piezoelectric sensor length decrease from 100  $\mu\text{m}$  to 25  $\mu\text{m}$ , the Q factor in air has been increased from  $\sim 120$  to  $\sim 170$  and from  $\sim 360$  to  $\sim 410$  for DC bias voltage of 2 V and 6 V respectively. The higher Q factor values achieved with shorter piezoelectric sensors is probably because of larger vibration amplitude induced. With the reduction of effective piezoelectric sensor area covering the beam, the mass loading held by the beam decreases and consequently a larger vibration amplitude can be induced under the same actuating conditions. The resulting



vibration amplitude increase and consequently the stored energy increase results in Q factor increase.

### **C. Piezoelectric port length influence on frequency tuning range**

The change of the piezoelectric sensor length has been found to affect the frequency tuning range. Figure 4 shows the resonant frequency shift for the devices with piezoelectric sensors integrated with lengths of 25, 50 and 100  $\mu\text{m}$  as a function of applied DC bias voltage. The resonant frequency tuning range of  $\sim 300,000$  ppm has been achieved using relatively low DC input bias voltage (2 V – 6 V). The decrease in resonant frequency detected as the DC bias voltage increases can be attributed to the increase of compressive stress in the beam, caused by the increase in thermal expansion of the structure as the temperature increases [14,15]. A wider resonant frequency tuning range has been observed for the devices with longer piezoelectric sensor length. From Figure 4, for DC bias voltage greater than 4 V, a relatively large difference in frequency shift is observable for different piezoelectric sensor lengths. The difference in the resonant frequency shift progressively increases with the DC bias voltage increase. In particular, as the piezoelectric sensor length increases from 25  $\mu\text{m}$  to 100  $\mu\text{m}$ , the frequency shift is observed to increase from  $\sim 120,000$  ppm to  $\sim 145,000$  (frequency shift increase of  $\sim 25,000$  ppm) at DC bias voltage of 5 V and from  $\sim 250,000$  ppm to  $\sim 295,000$  (frequency shift increase of  $\sim 45,000$  ppm) at DC bias voltage of 6 V. The larger influence of compressive stress may explain the wider resonant frequency tuning range obtained with the devices with longer piezoelectric sensor. By increasing the piezoelectric sensor length and positioning it close to the centre of the beam, the induced bending moment and shear force are increased, thus resulting in larger compressive stress compared to the case of the shorter

piezoelectric sensor positioned further away from the middle of the beam. In addition, as the DC bias voltage increase, induced temperature increase resulting in an additional increase of compressive stress and consequently in a larger decrease in resonant frequency.

## **V. CONCLUSIONS**

Piezoelectric sensors with different dimensions have been integrated on the top of electrothermally actuated 3C-SiC double-clamped beam resonators for studying the influence of piezoelectric sensor design on the device performance. The devices, actuated in the same operating conditions, with the shorter piezoelectric sensor have been shown to resonate at higher frequency with higher Q factor. The change of resonant frequency with the piezoelectric sensing length change is attributed to the change of structure's effective mass, while the change of Q factor is attributed to the change of vibration amplitude and consequently energy stored as the effective loading mass held by the beam has been changed. Moreover, the frequency tuning range has been shown to be affected by the piezoelectric sensor dimensions. With the piezoelectric sensor length increase and by positioning the sensor closer to the centre of the beam, a wider frequency tuning range has been obtained probably due to larger compressive stress induced in the beam. As the devices with the same design have been taken from the same die (fabrication related differences have been minimised) and tested in the same operating conditions, the results obtained can be used for improving the resonance performance of piezoelectrically transduced MEMS resonators.

## **ACKNOWLEDGMENTS**

One of us, B. Sviličić, acknowledges financial support of the Croatian Science Foundation.



## References

- [1] T. M. van Beek, R. Puers, J. Micromech. Microeng., 22 (2012) 013001-35.
- [2] A. Rahafrooz, S. Pourkamali, IEEE Trans. on Electron Devices, 54 (2011) 1205-1214.
- [3] R.B. Reichenbach, M. Zalalutdinov, J.M. Parpia, H.G. Craighead, IEEE Electron Device Lett., 27 (2006) 805-807.
- [4] J.H. Seo, O.Brand, Journal of Microelectromech. Systems, 17 (2008) 483 - 493.
- [5] B. Sviličić, E. Mastropaolo, B. Flynn, R. Cheung, IEEE Electron Device Lett., 33 (2012) 278-280.
- [6] R. Cheung, Silicon Carbide Micro Electromechanical Systems for Harsh Environments, Imperial College Press, London, 2006.
- [7] D.L. DeVoe, Sens. and Act. A, 88 (2001) 263-272.
- [8] P. Srinivasan, M. Spearing, J. Microelectromech. Syst., 17 (2008), 653-667.
- [9] L. Jiang, R. Cheung, J. Hedley, M. Hassan, A.J. Harris, J.S. Burdess, M. Mehregany, C.A. Zorman, Sens. and Act. A, 128 (2006), 376-386.
- [10] NovaSiC, <http://www.novasic.com>.
- [11] Inostek Inc., <http://www.inostek.com>.
- [12] E. Mastropaolo, I. Gual, G. Wood, A. Bunting, R. Cheung, J. of Vacuum Science and Technology B, 28 (2010), C6N18-C6N23.
- [13] L. Jiang, R. Cheung, R. Brown, A. Mount, J. of Appl. Physics, 93 (2003), 1376-1383.

- [14] C.S. Jun, X.M.H. Huang, M. Manolidis, C.A. Zorman, M. Mehregany, J. Hone, Nanotechnology, 17 (2006), 1506-1511.
- [15] E. Mastropaolo, G. Wood, I. Gual, P. Parmiter, R. Cheung; IEEE J. Microelectromech. Syst., 21 (2012), 811-821.

## Figure Captions

Figure 1. SEM image (a), top (b) and side (c) view schematics of the double-clamped 3C-SiC beam resonator, with the electrothermal actuator and piezoelectric sensor on top of the beam.

Figure 2. Transmission frequency response of one of the fabricated devices (a) and measured resonant frequency versus piezoelectric sensor length (b).

Figure 3. Measured Q factor in air versus tuning DC voltage with the piezoelectric sensor length  $L_{out}$  as a parameter.

Figure 4. Measured resonant frequency shift versus tuning DC voltage with the piezoelectric sensor length  $L_{out}$  as a parameter.

## Figures

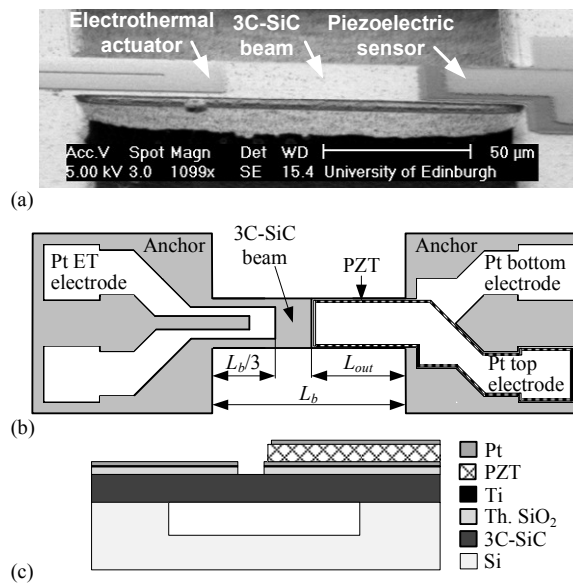


Figure 1

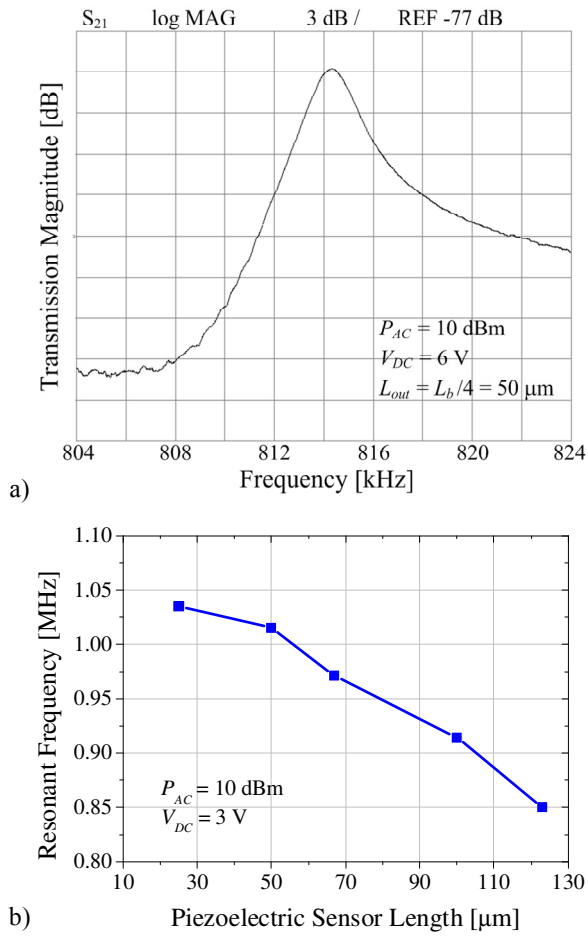


Figure 2



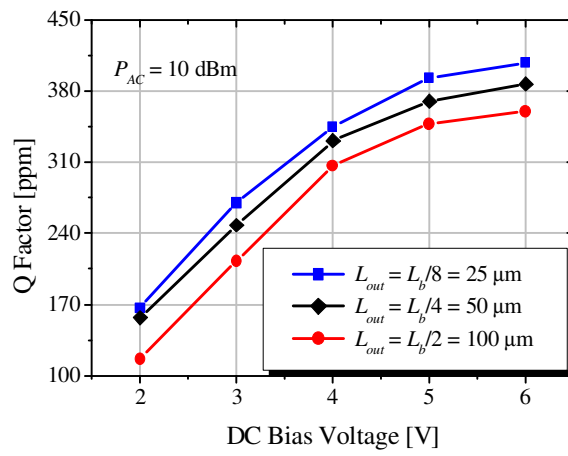


Figure 3

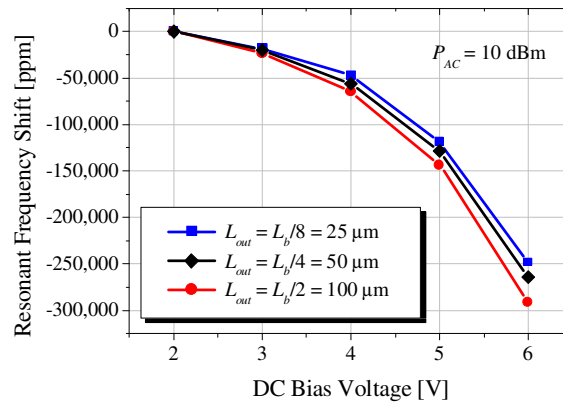


Figure 4